 CMC, vol.21, no.1, pp.65-86, 2011

Electromagnetic Shielding Effectiveness of Grid-Mesh Films Made of Polyaniline: a Numerical Approach

S. H. Kwon[1], B. R. Kim[2] and H. K. Lee[2,3]

Abstract: The electromagnetic shielding effectiveness of grid-mesh films made of polyaniline was numerically investigated, and the optimal size of the polyaniline grid was determined through numerical analyses. The permittivity of polyaniline was first determined from an inverse analysis based on experimental data. A series of numerical analyses were carried out with 225 polyaniline grid-mesh films of different thickness, spacing, and width, and the shielding effectiveness of every grid was examined. In addition to the numerical analysis, the transparency of the grid-mesh films and the amount of polyaniline material required to manufacture the unit grid area (1mx1m) were calculated. The optimal dimensions of the grid mesh were determined considering the following three factors: shielding effectiveness, transparency, and the required amount of polyaniline material.

Keywords: Polyaniline, Electromagnetic Shielding, Optical Transmission, Grid-Mesh Film, Optimal Grid Size

1 Introduction

In the last few years there has been intensive interest in electromagnetic (EM) wave shielding due to a dramatic increase in EM pollution, which can potentially lead to performance degradation or electromagnetic interference (EMI) of other electrical/electronic systems. A typical EM wave shielding system is comprised of entirely enclosed sheets or layers of electrically conductive metallic materials (e.g., steel or copper) (cf. Geetha et al., 2009). However, it is difficult to achieve both sufficient shielding effectiveness and visual accessibility (or transparency) with en-

[1] Department of Civil and Environmental Engineering, Myongji University, San 38-2, Namdong, Cheoin-gu, Yongin, Gyeonggi-do, 449-728, South Korea

[2] Department of Civil and Environmental Engineering, Korea Advanced Institute of Science and Technology, Guseong-dong, Yuseong-gu, Daejeon 305-701, South Korea

[3] Corresponding author. Tel.: +82 42 350 3623; Fax: +82 350 3610; *E-mail address*: leeh@kaist.ac.kr

tirely enclosed metallic shielding approaches (Hoeft et al., 1984). It is hence necessary to develop a new shielding system to resolve the existing problems.

Mesh structures are very attractive as EM wave shielding systems due to their visible light transmittance characteristics as well as their reduced weight per unit area compared to sheet types (Casey, 1988). In line with this, a variety of studies on metallic mesh structures have been carried out to design EM wave shielding systems (Mitsuishi et al., 1963; Vogel and Genzel, 1964; Ulrich, 1967; Wood et al., 1975; Bruneal et al., 1978; Möller et al., 2002; Roh et al., 2008). Although meshes made of metallic materials (e.g., steel, copper, and aluminum) offer high electromagnetic shielding effectiveness, they have various drawbacks such as heavy weight, corrosion susceptibility, and poor processibility (Yuping et al., 2005; Chen et al., 2007). Recently, as substitutes for these metallic materials, a variety of intrinsically conductive polymers (ICPs) having high dielectric constants have received a great deal of attention. These ICPs might provide solutions to the existing drawbacks due to their lightweight, corrosion resistance, good processibility, and simple conductivity control (Hoang et al., 2007; Nguema et al., 2008).

Polyaniline (PANI) is one of the most promising and versatile ICPs, affording interesting electrical characteristics along with good environmental stability (Abshinova et al., 2008; Jadhav and Puri, 2008; Bhadra et al., 2009). Due to these characteristics, PANI has been extensively investigated in relation to EM wave shielding. Refer to a series of studies on EM wave shielding characteristics of PANI carried out by many researchers (Mäkelä et al., 1997, 1999; Lee et al., 1999; Koul et al., 2000; Dhawan et al., 2002, 2003; Wang and Jing, 2005, 2007; Yuping et al., 2005; Bhadra et al., 2009; Kim et al., 2010, 2011). In particular, several studies have reported high dielectric constants, ranging from 10^2 to more than 10^5, of PANI composites (Joo et al., 1998; Dutta et al., 2002; Chwang et al., 2004; Yan and Goodson, 2006; Lu et al., 2007; Ho et al., 2008).

Grid-mesh films made of polyaniline might be a possible solution to easily achieve both the required EM shielding effectiveness and sufficient transparency. In this study, the electromagnetic shielding effectiveness of grid-mesh films made of polyaniline was numerically investigated, and the optimal size of the polyaniline grid was determined through numerical analyses. First, the permittivity of polyaniline was determined from an inverse analysis based on the experimental data. Numerical analyses were carried out with 225 polyaniline grid-mesh films of different thickness, spacing, and width, and the shielding effectiveness of every grid was examined. In addition to the numerical analysis, the transparency of the grid-mesh films and the amount of polyaniline material required to manufacture the same sectional area of the films were calculated. The optimal dimensions of the grid mesh were determined considering the following three factors: shielding effectiveness, trans-

parency, and the required amount of polyaniline material.

2 Electromagnetic properties of polyaniline

2.1 General

In a waveguide system, the radiated electromagnetic wave is generally scattered by an embedded material via reflection, absorption, and transmission. These forms of scattering are expressed as the scattering parameters, and are commonly called S-parameters (Kurokawa, 1965; Pozar, 2004; Kwon and Lee, 2009). The EM wave shielding effectiveness can be quantitatively expressed by these S-parameters (Wen and Chung, 2004). In particular, according to Nicholson and Ross (1970), the electromagnetic properties of materials can be obtained from S-parameter data. In the present study, the S-parameters are experimentally obtained from coaxial tests on PANI-coated films and the electromagnetic properties of PANI are calculated by S-parameter data. As the specimens for S-parameters, the PANI-coated films were manufactured by Elpani, Co. The details of the synthesis of PANI and manufacturing of the films can be found in Lee et al. (2005) and Kim et al. (2010).

2.2 Measurement of the S-parameters of polyaniline

The ASTM D 4935-99 standard method using a circular coaxial transmission line holder was performed to obtain the S-parameters of PANI. Although the ASTM D 4935-99 method is designed for EM wave shielding effectiveness, it can yield the S-parameters, which are used for calculating the electromagnetic properties of PANI. A frequency range of 30 MHz to 1.5 GHz was scanned. The scattering parameter S_{ij} is the ratio of the voltage at port i to the voltage at port j and can be expressed as a complex number. The set of S-parameters on specimens with different thickness of PANI (t=229, 366, 640, and 823 nm) is obtained from the tests. Figure 1 shows the schematic configuration of the coaxial test measurement system.

2.3 Calculation of the electromagnetic properties of polyaniline

The method for calculating the electromagnetic properties from S-parameters is described in Nicholson and Ross (1970). They report that scattering parameters S_{11} and S_{21} are related to the reflection coefficient (Γ) and transmission coefficient (T) and are expressed by the following (Nicholson and Ross, 1970)

$$S_{11} = \frac{(1-T^2)\Gamma}{1-\Gamma^2 T^2} \tag{1}$$

$$S_{21} = \frac{(1-\Gamma^2)T}{1-\Gamma^2 T^2} \tag{2}$$

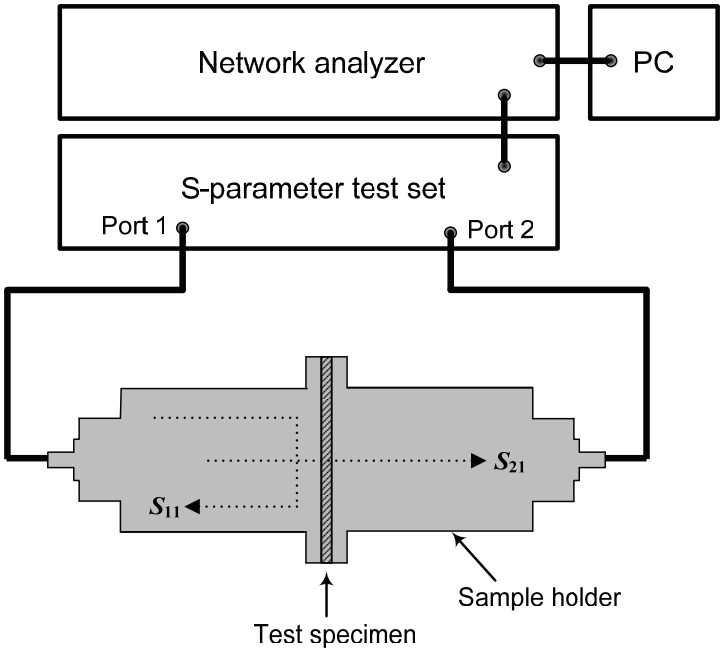

Figure 1: Schematic configuration of the coaxial test measurement system

with

$$\Gamma = \frac{\sqrt{\mu_R/\varepsilon_R} - 1}{\sqrt{\mu_R/\varepsilon_R} + 1} \tag{3}$$

$$T = \exp\left[-j(\omega/c)\sqrt{\mu_R/\varepsilon_R}t\right] \tag{4}$$

where ε_R and μ_R are the relative permittivity and permeability of the material, respectively. In addition, $j = \sqrt{-1}$, c is the speed of the wave under a vacuum, ω is the angular frequency, and t is the thickness of the material.

The electromagnetic properties ε_R and μ_R are complex functions with real and imaginary parts, expressed as $\varepsilon_R(\text{or } \mu_R) = \varepsilon_R'(\text{or } \mu_R') - j\varepsilon_R''(\text{or } \mu_R'')$, respectively (Nicholson and Ross, 1970; Baker-Jarvis et al., 1990). These properties can be determined from the S-parameters through an inverse analysis (Nicholson and Ross, 1970; Kwon and Lee, 2009). In the present study, nonlinear least square optimization using the Marquardt-Levenburg iteration kernel (Brown, 1970) is used for calculating the electromagnetic properties, optimally fitting the S-parameters measured from the experimental test. Figure 2 exhibits a flowchart describing iteration

algorithms used for determining the permittivity of PANI. It is noted that, for non-magnetic materials, the real and imaginary parts of permeability, μ_R' and μ_R'', are 1.0 and 0.0, respectively. The subscripts m and c in the flowchart denote "measured" and "calculated". In the present study, the real part of the relative permittivity of PANI is obtained as 5.961×10^5. Figure 3 shows the dielectric loss tangent of PANI according to the frequency calculated from the present optimization.

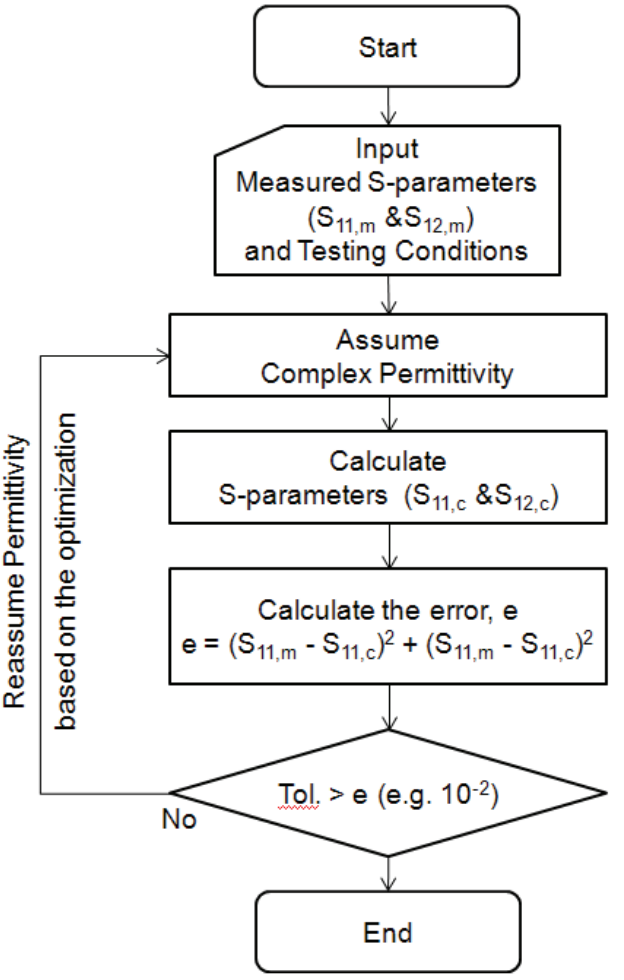

Figure 2: Flowchart describing iteration algorithms used for determining the permittivity of PANI

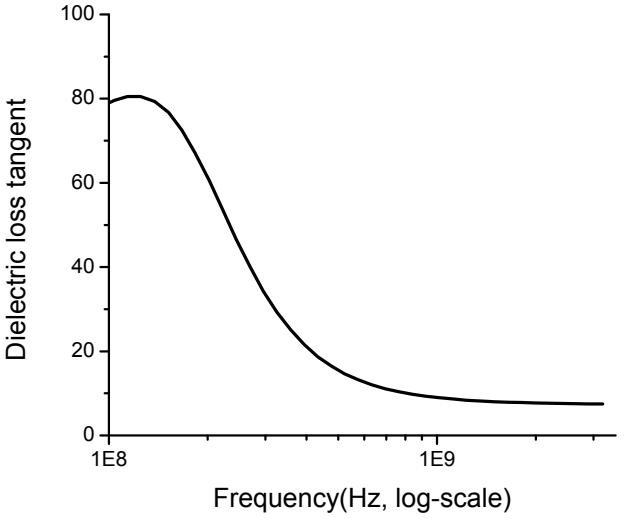

Figure 3: Dielectric loss tangent of PANI according to the frequency

3 Numerical analysis

3.1 General

In this study, the shielding effectiveness of PANI grid-mesh films with different thickness (t), spacing (s), and width (w) is numerically simulated. Figure 4 shows the unit cell of the PANI mesh for the numerical analysis and the specimen notation method according to a combination of analysis parameters. Here, 'T' and 'S' denote the thickness and spacing of the grid in millimeters, respectively. In addition, 'W' is the width of the grid and is expressed as the ratio of width to spacing. In order to determine the optimal grid size from the numerical simulation, the spacing and width of the grid are selected under the following assumptions (cf., Jacoby et al. (2009) and Zhang et al. (2009)): 1) the spacing of the grid is less than or equal to half of the frequency (λ); and 2) the ratio of width to spacing of the grid is determined as the approximate formula for optical transmission ($T_{optical} = (1 - w/l)^2$, where l=s-w). In particular, it is important that the optical transmission is not reduced below a minimum acceptable transparency (Sharples et al., 2001). Several references suggest that the minimum acceptable transparency ranges between 25% and 38%, and the standard transparency is in the range between 70% and 80% (cf. Boyce et al., 1995; Mathew et al., 1997; Sharples et al., 2001). Table 1 shows the analysis parameters of thickness, spacing, and width of the grid. In addition, Figure 5 presents a schematic description of the grid according to the ratio of width to

spacing (w/s=0.2, 0.1, 0.05, 0.01, 0.005). The total number of grid-meshes simulated in the analysis is 225; 5(thickness) x 9(Spacing) x 5(width).

Table 1: Analysis parameters of thickness, spacing, and width of the grid

Thickness, T (mm)	Relative width, W (width/spacing)	Spacing, S (mm)
0.001 (T1)	0.200 (W1)	50 (S1)
	0.100 (W2)	25 (S2)
	0.050 (W3)	10 (S3)
	0.010 (W4)	5.0 (S4)
	0.005 (W5)	2.5 (S5)
0.010 (T2)	0.200 (W1)	1.0 (S6)
	0.100 (W2)	0.5 (S7)
	0.050 (W3)	0.25 (S8)
	0.010 (W4)	0.10 (S9)
	0.005 (W5)	
0.020 (T3)	0.200 (W1)	
	0.100 (W2)	
	0.050 (W3)	
	0.010 (W4)	
	0.005 (W5)	
0.050 (T4)	0.200 (W1)	
	0.100 (W2)	
	0.050 (W3)	
	0.010 (W4)	
	0.005 (W5)	
0.100 (T5)	0.200 (W1)	
	0.100 (W2)	
	0.050 (W3)	
	0.010 (W4)	
	0.005 (W5)	

3.2 Modeling of PANI grid-mesh

A series of numerical simulations for the grid-mesh films were carried out with the commercial finite element (FE) program HFSS Ver. 11 (HFSS, 2008). The program utilizes a three-dimensional full-wave FE method to compute the electrical behavior of high-frequency and high-speed components (HFSS, 2008). Only the unit cell of the PANI grid was modeled in the analysis under the assumption that

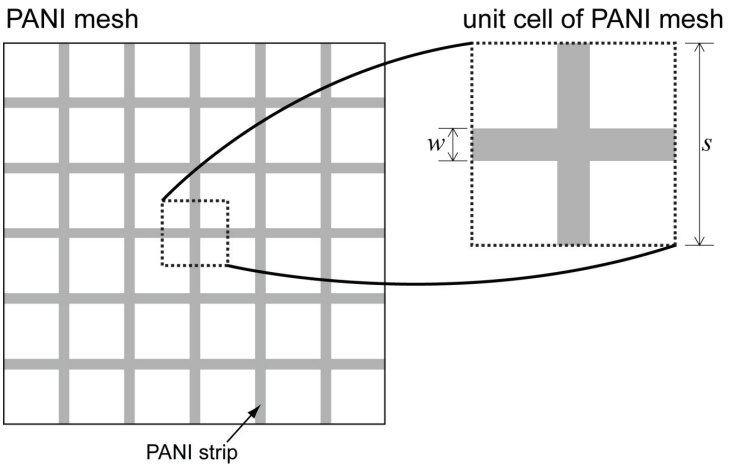

(a)

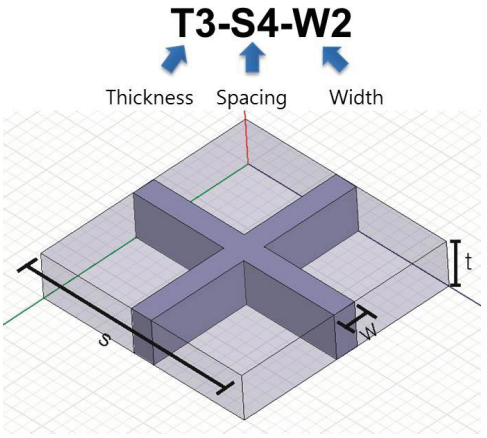

(b)

Figure 4: (a) Unit cell of the PANI mesh for numerical analysis and (b) specimen notation method according to a combination of analysis parameters

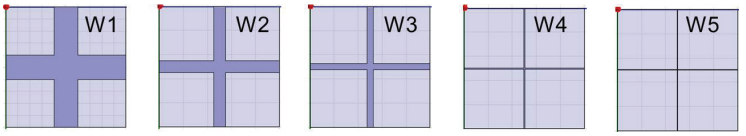

Figure 5: Schematic description of the grid according to the ratio of width to spacing (w/s=0.2, 0.1, 0.05, 0.01, 0.005)

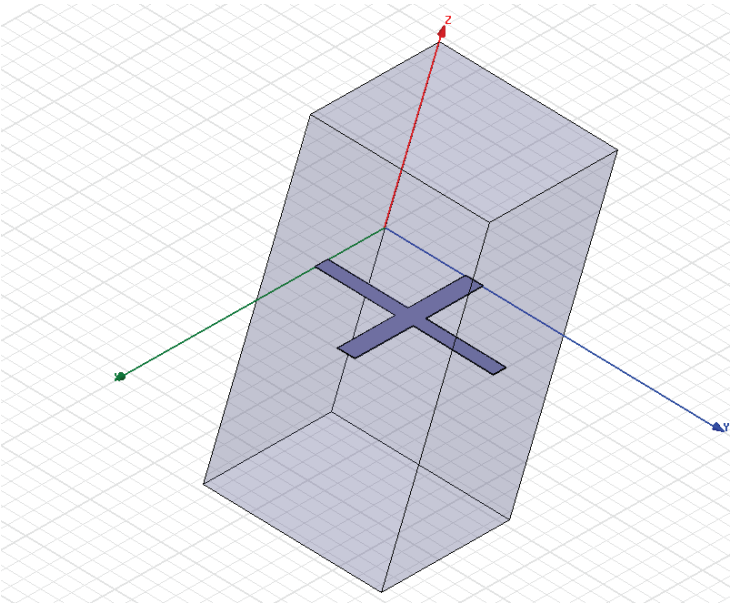

Figure 6: Description of the PANI grid unit cell of the infinitely repeated space in the FE program HFSS

the grid is infinite; that is, the unit cell is infinitely repeated in length and breadth, as shown in Figure 6. Two ports were placed at the top and the bottom surfaces of the specimen of Figure 6. The incident waves propagate from the upper port (Port 1), and the lower port (Port 2) accepts the waves transmitted through the grid. The periodic boundary conditions were set to the side faces so that the same electric and magnetic fields reappear on the opposite faces.

Figure 7 shows the simulated electromagnetic field distribution for the unit cell of the PANI grid at 3 GHz, and the red color represents higher intensity of the electric field. It can be seen from the figure that the electric field is symmetric and reappears in the opposite faces due to the periodic boundary conditions, and the PANI grid

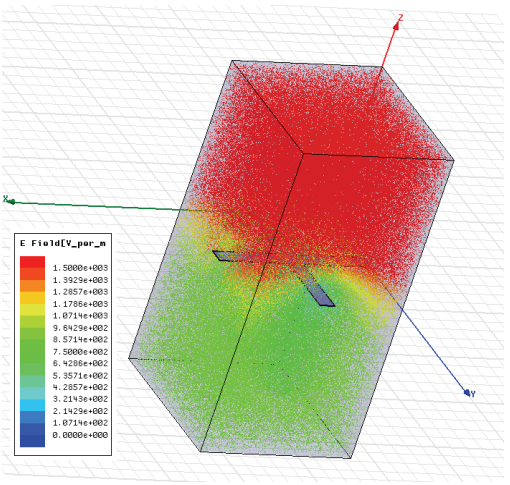

(a)

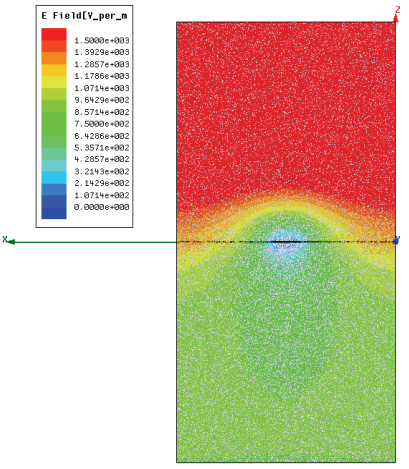

(b)

Figure 7: Electromagnetic field distribution for PANI mesh for an incident wave of 3 GHz (a) in three dimensional view and (b) in a cross-sectional view

prevents penetration of the EM wave.

The unit cell for all the simulation cases listed in Table 1 was modeled with tetrahedral elements and the convergence was checked on the basis of the difference between the S-parameters at the previous and current steps as the number of elements was increased. When the difference was less than a predefined tolerance, the analysis was performed with the last mesh refinement, decreasing the frequency from 3 GHz to 30 MHz.

4 Results and discussion

4.1 S-Parameters and Shielding Effectiveness

Figure 8 shows the S-parameters obtained from the numerical analysis. The S-parameters expressed in dB scale for several specimens are plotted over the frequency axis. It is shown in the figure that S_{11} increases and S_{21} decreases, respectively, with an increase of the frequency. This indicates that the proportion of the transmitted wave becomes higher as the frequency increases. Therefore, the shielding effectiveness of the grids can be calculated from the proportion of the transmitted wave at a frequency of 3 GHz, which is the maximum frequency in the numerical analysis.

Figure 9 shows the shielding effectiveness of the PANI grid-mesh films at 3 GHz. The S_{21} parameters at 3 GHz are plotted in the figure. It is shown in the figure that the shielding effectiveness increases with an increase of the thickness of grid. In addition, it is observed that the shielding effectiveness increases with a decrease of the spacing and an increase of the width of the grid, respectively.

4.2 Determination of optimal grid size

In general, the shielding effective values, that is, the S_{21} parameters, needed for many applications are at least -30 dB, i.e. the shielding would reduce the EM wave to as little as 0.1% of its initial strength (Greshham, 1988; Huang, 1995). Therefore, for determination of the optimal grid size, -30 dB was selected as the target value of the shielding effectiveness. Tables 2 to 6 show the shielding effectiveness and optical transmittance (transparency) of the specimens (T series girds) that satisfied the target value of the shielding effectiveness. In addition, the amount of PANI material used in manufacturing a grid of unit area (1 m $\times$ 1 m) was calculated and is expressed in the tables. The results in the tables could be used as fundamental data in determining the optimal grid size of PANI to shield EM waves while obtaining required optical transmittance.

In the present numerical analysis, the optimal grid size can be determined from the tables under the following conditions: 1) the shielding effectiveness exceeds

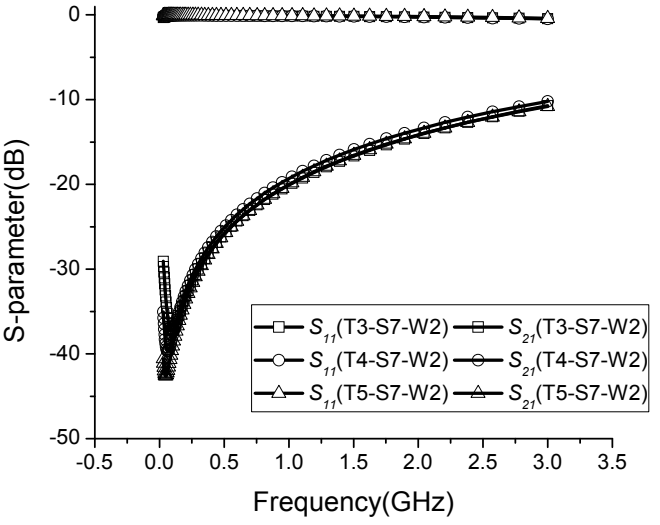

Figure 8: S-parameters obtained from the analysis

Table 2: Shielding effectiveness, transparency, and volume of PANI for T1 series grid (t=0.001 mm)

Specimens	**S (mm)**	**W (mm)**	S_{21} **(dB)**	**Transparency (%)**	**Volume of PANI in 1m×1m grid (mm^3)**
T1-S1-W1	0.1	0.02	-30.0	56.3	360
T1-S2-W1	0.25	0.05	-30.0	56.3	360

the target value (-30 dB); 2) higher optical transmittance (having values over 90% transparencies); and 3) a smaller amount of PANI used in manufacturing the grid. For thicknesses of 0.001mm and 0.01mm, as shown in Tables 2 and 3, no specimen provided more than 90% transparency. Tables 4 and 5 show that both more than 98 % transparency and the target shielding effectiveness (-30dB) can be obtained with PANI of 400 to 500 mm^3 per unit grid area (1m×1m) for grid thicknesses of 0.02mm and 0.05mm, respectively. However, for the thickness of 0.1 mm, 1,000 mm^3 per unit area (almost double that for the cases of thickness of 0.02mm and 0.05 mm) is needed to achieve the same level of transparency, although the shielding effectiveness is substantially enhanced. The following specimens are the grid size of PANI that satisfied with the optimal conditions: T3-S2-W4, T4-S1-W5, T4-S2-

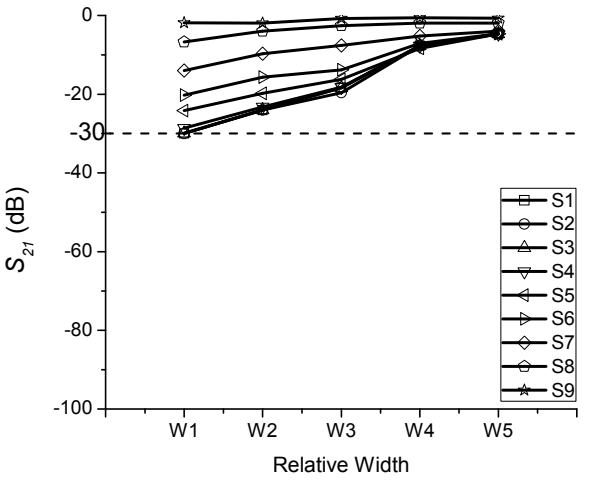

(a) T1 (0.001mm thickness)

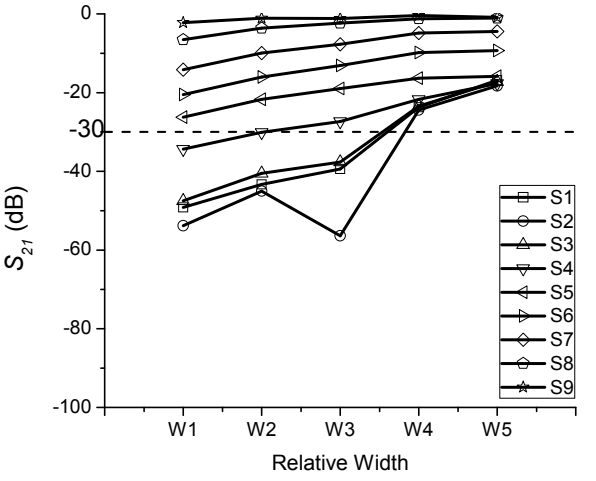

(b) T2 (0.01mm thickness)

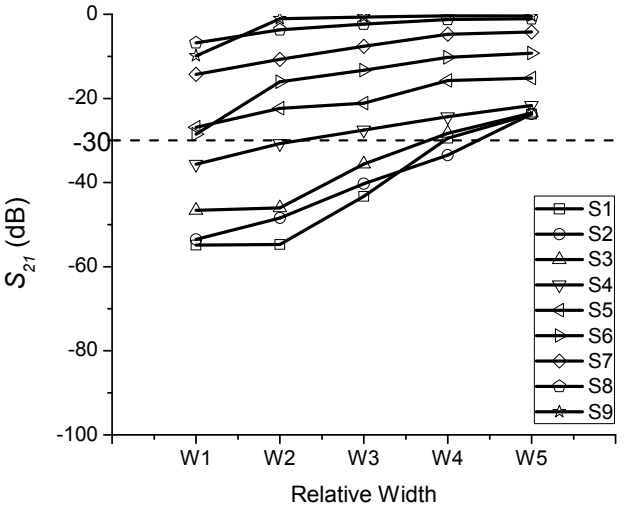

(c) T3 (0.02mm thickness)

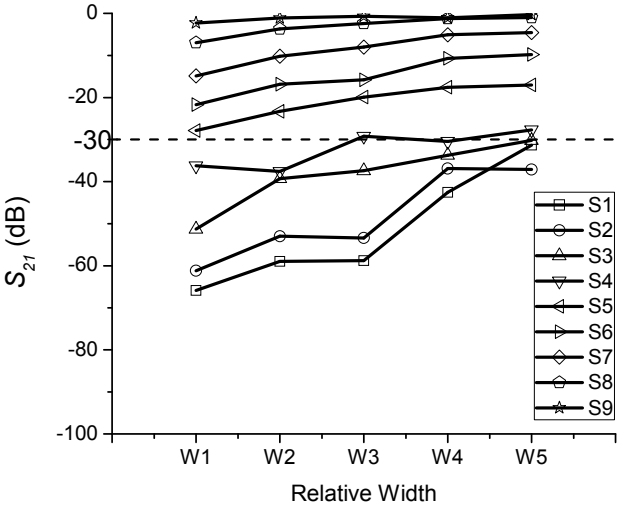

(d) T4 (0.05mm thickness)

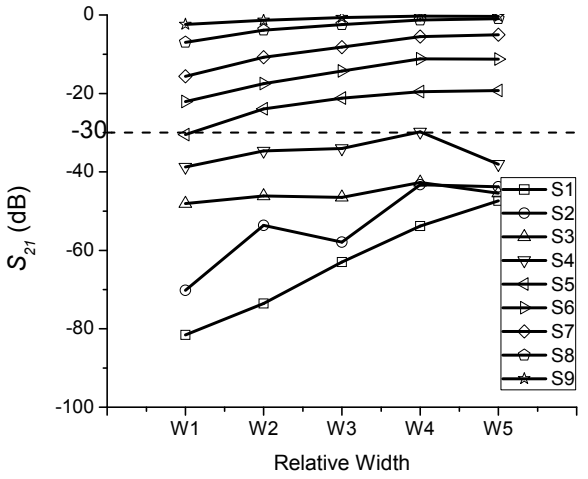

(e) T5 (0.1mm thickness)

Figure 9: Shielding effectiveness of the PANI grid-mesh films: (a) T1 series, (b) T2 series, (c) T3 series, (d) T4 series, and (e) T5 series (continued)

W5, and T4-S3-W5. In addition, thicknesses of 0.02 to 0.05 mm are relatively economically attractive.

Finally, it is worth noting that the obtained optimal values are suitable within the scope of the present numerical analysis. However, for cases beyond the scope of the present study, it is possible to predict the optimal grid size by interpolating the present results.

5 Concluding remarks

The effects of grid-mesh films with polyaniline on EM wave shielding according to different grid thicknesses, spacings, and widths have been presented in this study. In particular, the optimal grid size of PANI for effective EM wave shielding and sufficient transparency was determined. The permittivity of PANI was first calculated through an inverse analysis based on existing experimental data, and numerical studies on the suitable variables (thickness, spacing, and width of the grid) were carried out with 225 different PANI grid-mesh films. From the numerical analysis results, the following salient features were found.

Table 3: Shielding effectiveness, transparency, and volume of PANI for T2 series grid (t=0.01 mm)

Specimens	**S (mm)**	**W (mm)**	S_{21} **(dB)**	**Transparency (%)**	**Volume of PANI in 1m×1m grid (mm^3)**
T2-S1-W1	0.1	0.02	-49.2	56.3	3600
T2-S1-W2	0.1	0.01	-43.3	79.0	1900
T2-S1-W3	0.1	0.005	-39.4	89.8	975
T2-S2-W1	0.25	0.05	-53.8	56.3	3600
T2-S2-W2	0.25	0.025	-45.0	79.0	1900
T2-S2-W3	0.25	0.0125	-56.4	89.8	975
T2-S3-W1	0.5	0.1	-47.5	56.3	3600
T2-S3-W2	0.5	0.05	-40.5	79.0	1900
T2-S3-W3	0.5	0.025	-37.6	89.8	975
T2-S4-W1	1	0.2	-34.4	56.3	3600
T2-S4-W2	1	0.1	-30.1	79.0	1900

Table 4: Shielding effectiveness, transparency, and volume of PANI for T3 series grid (t=0.02 mm)

Specimens	**S (mm)**	**W (mm)**	S_{21} **(dB)**	**Transparency (%)**	**Volume of PANI in 1m×1m grid (mm^3)**
T3-S1-W1	0.1	0.02	-54.8	56.3	7200
T3-S1-W2	0.1	0.01	-54.7	79.0	3800
T3-S1-W3	0.1	0.005	-43.3	89.8	1950
T3-S2-W1	0.25	0.05	-53.5	56.3	7200
T3-S2-W2	0.25	0.025	-48.4	79.0	3800
T3-S2-W3	0.25	0.0125	-40.3	89.8	1950
T3-S2-W4	**0.25**	**0.0025**	**-33.5**	**98.0**	**398**
T3-S3-W1	0.5	0.1	-46.6	56.3	7200
T3-S3-W2	0.5	0.05	-46.0	79.0	3800
T3-S3-W3	0.5	0.025	-35.6	89.8	1950
T3-S4-W1	1	0.2	-35.6	56.3	7200
T3-S4-W2	1	0.1	-30.7	79.0	3800

Table 5: Shielding effectiveness, transparency, and volume of PANI for T4 series grid (t=0.05 mm)

Specimens	**S (mm)**	**W (mm)**	S_{21} **(dB)**	**Transparency (%)**	**Volume of PANI in 1m×1m grid (mm^3)**
T4-S1-W1	0.1	0.02	-65.9	56.3	18000
T4-S1-W2	0.1	0.01	-59.0	79.0	9500
T4-S1-W3	0.1	0.005	-58.8	89.8	4875
T4-S1-W4	0.1	0.001	-42.6	98.0	995
T4-S1-W5	**0.1**	**0.0005**	**-31.3**	**99.0**	**499**
T4-S2-W1	0.25	0.05	-61.2	56.3	18000
T4-S2-W2	0.25	0.025	-53.0	79.0	9500
T4-S2-W3	0.25	0.0125	-53.4	89.8	4875
T4-S2-W4	0.25	0.0025	-36.9	98.0	995
T4-S2-W5	**0.25**	**0.00125**	**-37.1**	**99.0**	**499**
T4-S3-W1	0.5	0.1	-51.3	56.3	18000
T4-S3-W2	0.5	0.05	-39.3	79.0	9500
T4-S3-W3	0.5	0.025	-37.4	89.8	4875
T4-S3-W4	0.5	0.005	-33.7	98.0	995
T4-S3-W5	**0.5**	**0.0025**	**-30.2**	**99.0**	**499**
T4-S4-W1	1	0.2	-36.2	56.3	18000
T4-S4-W2	1	0.1	-37.6	79.0	9500
T4-S4-W4	1	0.01	-30.5	98.0	995

(1) The shielding effectiveness increased with an increase of the thickness and width of grid and a decrease of the spacing of the grid.

(2) The T3-S2-W4, T4-S1-W5, T4-S2-W5, and T4-S3-W5 specimens were the grid size of PANI that satisfied with the optimal conditions.

(3) The economic range of the grid thickness was found to be from 0.02 to 0.05 mm, and the optimal dimensions of PANI grids to achieve both -30dB shielding effectiveness and transparency exceeding 98% were suggested.

(4) The obtained optimal values are suitable within the scope of the present numerical analysis. However, for cases beyond the scope of the present study, it is possible to predict the optimal grid size by interpolating the present results

In conclusion, the results of the present study showed the potential use of PANI grid-mesh films as an EM wave shielding systems. In addition, the relatively rea-

Table 6: Shielding effectiveness, transparency, and volume of PANI for T5 series grid (t=0.1 mm)

Specimens	**S (mm)**	**W (mm)**	S_{21} **(dB)**	**Transparency (%)**	**Volume of PANI in 1m×1m grid (mm^3)**
T5-S1-W1	0.1	0.02	-81.5	56.3	36000
T5-S1-W2	0.1	0.01	-73.6	79.0	19000
T5-S1-W3	0.1	0.005	-63.0	89.8	9750
T5-S1-W4	0.1	0.001	-53.8	98.0	1990
T5-S1-W5	0.1	0.0005	**-47.4**	**99.0**	**998**
T5-S2-W1	0.25	0.05	-70.2	56.3	36000
T5-S2-W2	0.25	0.025	-53.6	79.0	19000
T5-S2-W3	0.25	0.0125	-57.9	89.8	9750
T5-S2-W4	0.25	0.0025	-43.2	98.0	1990
T5-S2-W5	0.25	0.00125	**-43.8**	**99.0**	**998**
T5-S3-W1	0.5	0.1	-48.1	56.3	36000
T5-S3-W2	0.5	0.05	-46.1	79.0	19000
T5-S3-W3	0.5	0.025	-46.5	89.8	9750
T5-S3-W4	0.5	0.005	-42.7	98.0	1990
T5-S3-W5	0.5	0.0025	**-45.4**	**99.0**	**998**
T5-S4-W1	1	0.2	-38.8	56.3	36000
T5-S4-W2	1	0.1	-34.7	79.0	19000
T5-S4-W3	1	0.05	-34.0	89.8	9750
T5-S4-W5	1	0.005	**-38.0**	**99.0**	**998**
T5-S5-W1	2.5	0.5	-30.5	56.3	36000

sonable grid size of PANI for effective EM wave shielding and sufficient transparency was determined in the present study. However, further experimental works based on the present results need to be carried out to for field applications of PANI grid-mesh films.

Acknowledgement: This research was supported by the IT R&D program of MKE/IITA [2008-F-044-01, Development of new IT convergence technology for smart building to improve the environment of electromagnetic waves, sound, and building] and by a Korea Science and Engineering Foundation (KOSEF) grant funded by the Korean government (MEST20090080587).

References

Abshinova, M.A., Kazantseva, N.E., Sáha, P., Sapurina, I., Koválová, J., Stejskal, J. (2008): The enhancement of the oxidation resistance of carbonyl iron by polyaniline coating and consequent changes in electromagnetic properties, *Polymer Degradation and Stability*, Vol. 93, No. 10, pp. 1826-1831.

Baker-Jarvis, J., Vanzura, E.J., Kissick, W.A. (1990): Improved technique for determining complex permittivity with the transmission/reflection method, *IEEE Transactions on Microwave Theory and Techniques*, Vol. 38, No. 8, pp. 1096-1103.

Bhadra, S., Singha, N.K., Khastgir, D. (2009): Dielectric properties and EMI shielding efficiency of polyaniline and ethylene 1-octene based semi-conducting composites, *Current Applied Physics*, Vol. 9, No. 2, pp. 396-403.

Boyce, P., Eklund, N., Mangum, S., Saalfield, C., Tang, L. (1995): Minimum acceptable transmittance of glazing, *Lighting Research and Technology*, Vol. 27, No. 3, pp. 145-152.

Brown, K.M. (1970): Derivative-Free Analogues of the Levenberg, Marquardt and Gauss Algorithms for Nonlinear Lest Square Approximations, IBM, Philadelphia Scientific Center Technical Report, No. 320-2994.

Bruneal, J.L., Belland, P., Véron, D. (1978): A CW DCN waveguide laser of high volumetric efficiency, *Optic Communication*, Vol. 24, No. 3, pp. 259-264.

Casey, K.F. (1988): Electromagnetic shielding behavior of wire-mesh screens, *IEEE Transactions on Electromagnetic Compatibility*, Vol. 30, No. 3, pp. 298-306.

Chen, H.C., Lee, K.C., Lin, J.H., Koch, M. (2007): Fabrication of conductive woven fabric and analysis of electromagnetic shielding via measurement and empirical equation, *Journal of Materials Processing Technology*, Vol. 184, Nos. 1-3, pp. 124-130.

Chwang, C.P., Liu, C.D., Huang, S.W., Chao, D.Y., Lee, S.N. (2004): Synthesis and characterization of high dielectric constant polyaniline/polyurethane blends, *Synthetic Metals*, Vol. 142, Nos. 1-3, pp. 275-281.

Dhawan, S.K., Singh, N., Venkatachalam, S. (2002): Shielding effectiveness of conducting polyaniline coated fabrics at 101 GHz, *Synthetic Metals*, Vol. 125, No. 3, pp. 389-393.

Dhawan, S.K., Singh, N., Rodrigues, D. (2003): Electromagnetic shielding behaviour of conducting polyaniline composites, *Science and Technology of Advanced Materials*, Vol. 4, No. 2, pp. 105-113.

Dutta, P., Biswas, S., Subodh Kumar De (2002): Dielectric relaxation in polyaniline-

polyvinyl alcohol composites, *Materials Research Bulletin*, Vol. 37, No. 1, pp. 193-200.

Geetha, S., Satheesh Kumer, K.K., Rao, C.R.K., Vijayan, M., Trivedi, D.C. (2009): EMI shielding: methods and materials-a review, *Journal of Applied Polymer Science*, Vol. 112, No. 4, pp. 2073-2086.

Greshham, R.M. (1988): EMI/RFI shielding of plastics, Plastic Surface Finishing, pp. 63-69.

HFSS. (2008): High Frequency Structure Simulation, Ansoft Inc.

Ho, C.H., Liu, C.D., Hsieh, C.H., Hsieh, K.H., Lee, S.N. (2008): High dielectric constant polyaniline/poly(acrylic acid) composites prepared by in situ polymerization, *Synthetic Metals*, Vol. 158, No. 15, pp. 630-637.

Hoang, N.H., Wojkiewicz, J.L., Miane, J.L., Biscarro, R.S. (2007): Lightweight electromagnetic shields using optimized polyaniline composites in the microwave band, *Polymers for Advanced Technology*, Vol. 18, No. 4, pp. 257-262.

Hoeft, L.O., Karaskiewicz, R.J., Hofstra, J.S. (1984): Measured surface magnetic field attenuation of shielded windows and wire mesh over an electrically small enclosure, *IEEE Transactions on Nuclear Science*, Vol. NS-31, No. 6, pp. 1312-1315.

Huang, J.C. (1995): EMI shielding plastics: a review, *Advances in Polymer Technology*, Vol. 14, No. 2, pp. 137-150.

Jacoby, K.T., Pieratt, M.W., Halman, J.I., Ramsey, K.A. (2009): Predicted and measured EMI shielding effectiveness of a metallic mesh coating on a sapphire window over a broad frequency range, In: Window and Dome Technologies and Materials XI (editor: R.W. Tustison), Vol. 7302, p. 7302OX.

Jadhav, S.V. and Puri, V. (2008): Microwave absorption and permittivity of polyaniline thin films using overlay technique, *Microelectronics Journal*, Vol. 39, No. 12, pp. 1472-1475.

Joo, J., Long, S.M., Pouget, J.P., Oh, E.J., MacDiarmid, A.G., Epstein, A.J. (1998): Charge transport of the mesoscopic metallic state in partially crystalline polyanilines, *Physical Review B. Condensed Matter and Materials Physics*, Vol. 57, No. 16, pp. 9567-9580.

Kim, B.R., Lee, H.K., Kim, E., Lee, S.H. (2010): Intrinsic electromagnetic radiation shielding/absorbing characteristics of polyaniline-coated transparent thin films, *Synthetic Metals*, Vol. 160, Nos. 17-18, pp. 1838-1842.

Kim, B.R., Lee, H.K., Park, S.H., Kim, H.K. (2011): Electromagnetic interference shielding characteristics and shielding effectiveness of polyaniline-coated films, *Thin Solid Films*, Vol. 519, No. 11, pp. 3492-3496.

Koul, S., Chandra, R., Dhawan, S.K. (2000): Conducting polyaniline composite for ESD and EMI at 101 GHz, *Polymer*, Vol. 41, No. 26, pp. 9305-9310.

Kurokawa, K. (1965): Power waves and the scattering matrix, IEEE Transactions on Microwave Theory and Techniques, Vol. 13, No. 2, pp. 194-202.

Kwon, S.H. and Lee, H.K. (2009): A computational approach to investigate electromagnetic shielding effectiveness of steel fiber reinforced mortar, Computers, Materials, & Continua, Vol. 12, No. 3, pp. 197-222.

Lee, C.Y., Song, H.G., Jang, K.S., Oh, E.J., Epstein, A.J., Joo, J. (1999): Electromagnetic interference shielding efficiency of polyaniline mixtures and multilayer films, *Synthetic Metals*, Vol. 102, Nos. 1-3, pp. 1346-1349.

Lee, S.H., Lee, D.H., Lee, K., Lee, C.W. (2005): High-performance polyaniline prepared via polymerization in a self-stabilized dispersion, Advanced Functional Materials, Vol. 15, No. 9, pp. 1495-1500.

Lu, J., Moon, K.S., Kim, B.K., Wong, C.P. (2007): High dielectric constant polyaniline/epoxy composites via in situ polymerization for embedded capacitor applications, *Polymer*, Vol. 48, No. 6, pp. 1510-1516.

Mäkelä, T., Pienimaa, S., Taka, T., Jussila, S., Isotalo, H. (1997): Thin polyaniline films in EMI shielding, *Synthetic Metals*, Vol. 85, Nos. 1-3, pp. 1335-1336.

Mäkelä, T., Sten, J., Hujanen, A., Isotalo, H. (1999): High frequency polyaniline shields, *Synthetic Metals*, Vol. 101, Nos. 1-3, p. 707.

Mathew, J.G.H., Sapers, S.P., Cumbo, M.J., O'Brien, N.A., Sargent, R.B., Raksha, V.P., Lahaderne, R.B., Hichwa, B.P. (1997): Large area electrochromics for architectural applications, *Journal of Non-Crystalline Solids*, Vol. 218, No. 2, pp. 342-346.

Mitsuishi, A., Otsuka, Y., Fujita, S., Yoshinaga, H. (1963): Metal mesh filters in the far infrared region, *Japanese Journal of Applied Physics*, Vol. 2, No. 9, pp. 574-577.

Möller, K.D., Sternberg, O., Grebel, H., Stewart, K.P. (2002): Near-field effects in multilayer inductive metal meshes, *Applied Optics*, Vol. 41, No. 10, pp. 1942-1948.

Nguema, E., Vigneras, V., Miane, J.L., Mounaix, P. (2008): Dielectric properties of conducting polyaniline films by THz time-domain spectroscopy, *European Polymer Journal*, Vol. 44, No. 1, pp. 124-129.

Nicolson, A.M. and Ross, G.F. (1970): Measurement of the intrinsic properties of materials by time-domain techniques, *IEEE Transactions on Instrumentation and Measurement*, Vol. IM-19, No. 4, pp. 377-382.

Pozar, D.M. (2004): Microwave Engineering, Third Edition, John Wiley & Sons,

Inc.

Roh, J.S., Chi, Y.S., Kang, T.J., Nam, S.W. (2008): Electromagnetic shielding effectiveness of multifunctional metal composite fabrics, *Textile Research Journal*, Vol. 78, No. 9, pp. 825-835.

Sharples, S., Stewart, L., Tregenza, P.R. (2001): Glazing daylight transmittances: a field survey of windows in urban area, *Building and Environment*, Vol. 36, No. 4, pp. 503-509.

Ulrich, R. (1976): Far-infrared properties of metallic mesh and its complementary structure, *Infrared Physics*, Vol. 7, No. 1, pp. 37-55.

Vogel, P. and Genzel, L. (1964): Transmission and reflection of metallic mesh in the far infrared, *Infrared Physics*, Vol. 4, No. 4, pp. 257-262.

Wang, Y. and Jing, X. (2005): Intrinsically conducting polymers for electromagnetic interference shielding, *Polymers for Advanced Technologies*, Vol. 16, No. 4, pp. 344-351.

Wang, Y. and Jing, X. (2007): Transparent conductive thin films based on polyaniline nanofibers, Materials Science and Engineering: B. *Advanced Functional Solid-State Materials*, Vol. 138, No. 1, pp. 95-100.

Wen, S. and Chung, D.D.L. (2004): Electromagnetic interference shielding reaching 70 dB in steel fiber cement, *Cement and Concrete Research*, Vol. 34, No. 2, pp. 329-332.

Wood, R.A., Brignall, N., Pidgeon, C.R., Berkdar, F.A. (1975): An optically pumped waveguide laser with mesh reflectors, *Optic Communication*, Vol. 14, No. 3, pp. 301-303.

Yan, X.Z. and Goodson, T. (2006): High dielectric hyperbranched polyaniline materials, *The Journal of Physical Chemistry B*, Vol. 110, No. 30, pp. 14667-14672.

Yuping, D., Shunhua, L., Hongtao, G. (2005): Investigation of electrical conductivity and electromagnetic shielding effectiveness of polyaniline composites, *Science and Technology of Advanced Materials*, Vol. 6, No. 5, pp. 513-518.

Zhang, S., Jin, L., Wu, Y., Wu, Q., Li, L.W. (2009): A novel transparent carbon nanotube film for radio frequency electromagnetic shielding applications, Proceedings of Microwave Conference, APMC 2009, Asia Pacific, pp. 1281-1284.